Ferrocene-Modified Purines as Potential Electrochemical Markers: Synthesis, Crystal Structures, Electrochemistry and Cytostatic Activity of (Ferrocenylethynyl)- and (Ferrocenylethyl)purines

Michal Hocek,*[a] Petr Štěpnička,*[b] Jiří Ludvík,[c] Ivana Císařová,[b] Ivan Votruba,[a] David Řeha,[c, d] and Pavel Hobza[c, d]

Abstract: Palladium-catalyzed Sonogashira cross-coupling reactions of halopurines 9-benzyl-6-chloropurine (**2a**), 9-benzyl-8-bromoadenine (**2b**), and 9-benzyl-2-chloroadenine (**2c**) with ethynylferrocene (**1**) gave the corresponding (ferrocenylethynyl)purines **3a–c** in moderate to good yields. Catalytic hydrogenation of these alkynes over Pd/C afforded the respective saturated [2-(ferrocenyl)ethyl]purines **4a–c**. The crystal structures **3a**, **3b**, **4a** and **4b** as determined by X-ray diffraction show interesting solid-state interactions, markedly different for purines **3a** and **4a** on one hand and adenines **3b** and **4b** that possess a free amino group on the other. Electrochemistry of electrochemically labelled purines **3** and **4** has been studied by voltammetry and cyclic voltammetry on platinum disc electrode and the experimental oxidation potentials were confirmed and explained by ionization potentials from theoretical DFT calculations. Several compounds of this series exhibited a considerable cytostatic effect.

Keywords: ab initio calculations · cytostatic activity · electrochemistry · ferrocenes · nucleobases · purines · solid-state assembly · X-ray diffraction

Introduction

Purines bearing carbon substituents in positions 2, 6 or 8 possess a broad spectrum of biological activities.[1] For instance, 2-alkynyladenosines constitute an important class of adenosine A_2-receptors agonists[2] that are investigated as potential therapeutic agents for the treatment of cardiovascular problems, inflammation, Parkinson's disease, schizophrenia, diabetes. On the other hand, 8-aryl- and 8-alkenyl-1,3,7-trimethylxanthines are antagonists of A_1 and A_2 receptors[3] whereas 8-alkynyladenosines are selective antagonists to A_3-receptor.[4] 6-(Arylalkynyl)-, 6-(arylalkenyl)- and 6-(arylalkyl)purines show cytokinin[5] and antioxidant[6] activity, while 9-benzyl-6-arylpurines exhibit antimycobacterial, antibacterial and cytotoxic effect.[7] 6-Aryl and 6-(arylakyl)purine ribonucleosides[8] as well as some arylalkynyl-9-benzylpurines[9] display significant cytostatic activity.

An investigation of the underlying biological processes and modeling of their mechanisms can be facilitated by the use of electrochemically-modified compounds and following their electrochemical properties. This approach relies on mutual electronic interactions of two parts of a molecular system where an incorporated redox probe is able to reflect electronic changes that occur in the other part of the molecule (induced by, e.g., a redox process, host–guest interaction, acid–base equilibria, ion pairing) by its changed elec-

[a] Dr. M. Hocek, Dr. I. Votruba
Institute of Organic Chemistry and Biochemistry
Academy of Sciences of the Czech Republic, Flemingovo nám. 2
16610 Prague 6 (Czech Republic)
Fax: (+420) 233-331-271
E-mail: hocek@uochb.cas.cz

[b] Dr. P. Štěpnička, Dr. I. Císařová
Department of Inorganic Chemistry, Faculty of Science
Charles University, Hlavova 2030
12840 Prague 2 (Czech Republic)
Fax: (+420) 221-951-253
E-mail: stepnic@natur.cuni.cz
cisarova@natur.cuni.cz

[c] Dr. J. Ludvík, D. Řeha, Prof. P. Hobza
J. Heyrovský Institute of Physical Chemistry
Academy of Sciences of the Czech Republic, Dolejškova 3
18223 Prague 8 (Czech Republic)
E-mail: jiri.ludvik@jh-inst.cas.cz
david.reha@jh-inst.cas.cz
hobza@indy.jh-inst.cas.cz

[d] D. Řeha, Prof. P. Hobza
Center for Complex Molecular Systems and Biomolecules
Dolejškova 3, 182 23 Prague (Czech Republic)
E-mail: david.reha@jh-inst.cas.cz
hobza@indy.jh-inst.cas.cz

Supporting information for this article is available on the WWW under http://www.chemeurj.org/ or from the author.

DOI: 10.1002/chem.200305621

trochemical response. The prerequisite is that the redox probe interacts electronically with the parent molecule, forming usually an electronically delocalized system via a conjugated or coordination linker. Then, the redox properties of the probe are perturbed by changes taking place at the parent molecule and can be quantified by electrochemical methods.

Ferrocene is a very useful electrochemically active label for important classes of biologically relevant compounds, and conjugates of nucleobases, nucleosides and nucleic acids with ferrocene represent an attractive target. Thus 2′-*O*-ferrocenylalkyl nucleotides have been prepared[10] and incorporated into oligonucleotides as a probe for single-base mutations.[11] 5-Ferrocenylethynylpyrimidine nucleosides were synthesized by Sonogashira coupling of 5-iodopyrimidines with ethynylferrocene (**1**) and incorporated into DNA as electroactive redox markers.[12] Very recently, during the course of our work, the Sonogashira coupling of **1** was used[13] for labelling of some biomolecules including 8-bromoadenosine and 8-bromo-9-butyladenine.

Despite the recent related work,[13] we wish to report herein our study on the Sonogashira cross-coupling between ethynylferrocene (**1**) and 2-, 6- and 8-halopurines leading to the corresponding (ferrocenylethynyl)purines and their hydrogenation to give the saturated derivatives. In the resulting two types of the modified purines, the ferrocene unit is connected either via a conjugated ethynediyl or a non-conjugated ethan-1,2-diyl bridge. Since the ferrocene moiety acts not only as an electrochemical label but also as a defined, bulky hydrophobic substituent, the molecular structures, electrochemistry and biological activity of the compounds have been studied.

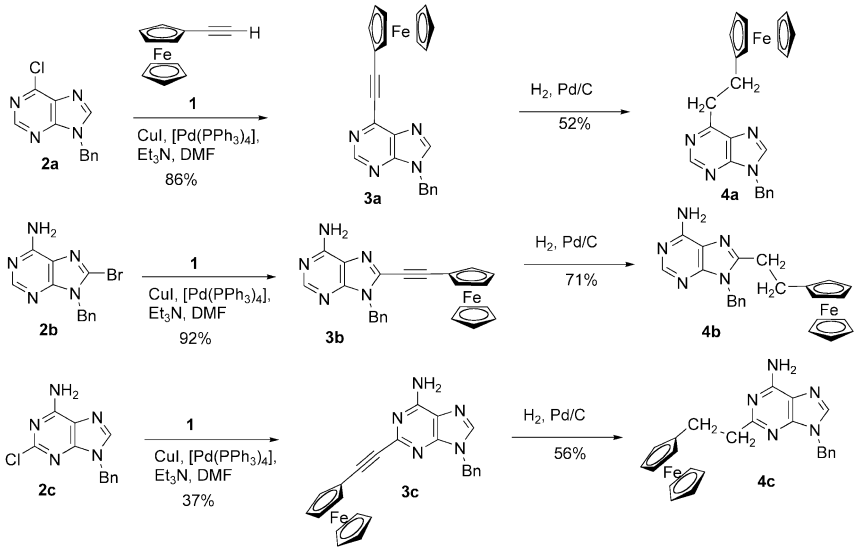

Scheme 1.

Results and Discussion

Synthesis: Cross-coupling reactions are the most practical methodology[1] for an introduction of a carbon substituent into positions 2, 6 and 8 of the purine moiety. Among them, the Sonogashira reaction of terminal alkynes with halopurines is the method of choice for the introduction of an alkynyl group.[4,5,9] Cross-couplings of ethynylferrocene with 5-iodopyrimidines[12] and, recently, also with 8-bromoadenosine[13] have been used for the synthesis of 5-(ferrocenylethynyl)pyrimidines and 8-(ferrocenylethynyl)purines, respectively.

We have employed ethynylferrocene (**1**) in the series of cross-coupling reactions (see Scheme 1) with 9-benzyl protected 6-chloropurine (**2a**), 8-bromoadenine (**2b**) and 2-chloroadenine (**2c**). The reactions were performed under the standard conditions at 120 °C in DMF and triethylamine in the presence of catalytic amounts of CuI and $[Pd(PPh_3)_4]$. The reactions in the positions 6 or 8 (with compounds **2a** and **2b**) proceeded smoothly to give the ferrocenylethynylpurines **3a** and **3b** in 86 and 92 %, respectively. A similar reaction with 2-chloroadenine **2c** was substantially slower, affording 2-(ferrocenylethynyl)adenine **3c** in only a moderate yield of 37 % even after prolonged reaction time (36 h). However, as a large part of the unreacted starting material (40 %) is easily recovered from the reaction mixture by column chromatography, even this rather low-yielding reaction could be synthetically useful.

The ferrocenylethynylpurines **3a–c** have been further hydrogenated over 10 % Pd/C under atmospheric pressure in a mixture of dioxane, ethanol and acetic acid. The reactions were relatively slow, giving the corresponding (2-ferrocenylethyl)purines **4a–c** in 52, 71 and 56 % isolated yield, respectively. Under the reaction conditions, the benzyl groups were not cleaved-off. Some unidentified oligo-/polymeric side-products were lost during purification by column chromatography.

X-Ray crystallography: The solid-state structures of **3a**, **3b**, **4a** have been determined by X-ray diffraction (Figures 1, 2 and 3). Structural parameters of the purine core (Table 1) are unexceptional and do not differ much within the whole series. However, differences are observed for the ferrocenylated side arm: the rod-like ethynediyl linking group in **3a** and **3b** brings the ferrocenyl group into a defined position, allowing it only to rotate along the triple bond axis. The reduction of the ethynediyl (**3a**) to a flexible ethane-1,2-diyl group (**4a**) changes the geometry and conformation of the ferrocenylated pendant, leaving the other molecular parts nearly intact: the C6–C10 bond in **4a** is elongated by about

5% compared with the parent **3a** due to an interrupted conjugation of the purine and ferrocenyl groups, and the ferrocenyl substituent adopts a position nearly perpendicular to the purine plane. The orientation of the aromatic planes can be influenced by their involvement in intermolecular interactions, see below.

Far more interesting are the solid-state packings of these compounds and also of **4b**. Its structure was determined as well but with a rather low precision (albeit unambiguously) due to a poor crystal quality (the molecular parameters of **4b** do not differ significantly from the above-mentioned compounds and will not be discussed). The molecules of **3a** assemble via offset π···π interactions of the six-membered heterocyclic rings, which are by-symmetry-parallel, lying across the crystallographic inversion centres [Cg···Cg & sym(1−*x*, −*y*, 1−*z*): 3.3135(8) Å, interplanar distance 3.25 Å; Cg denotes the ring centroid] (Figure 4). The structure is further aided by C−H···π-ring interactions between the ferrocenyl unit and phenyl group of a neighbouring molecule [C16−H(16)···Cg(Ph) & sym($x+\frac{1}{2}$, $\frac{1}{2}-y$, $z-\frac{1}{2}$): Cg···C16 3.434(2) Å, C16−H16···Cg 163°]. The structure of **4a** features similar interactions (Figure S1 in the Supporting Information): the molecules associate via π···π interactions of parallel six-membered heterocyclic rings [Cg(Pur^6)···Cg(Pur^6) & sym(2−*x*, 1−*y*, −*z*) 3.4003(8) Å, interplanar distance 3.23 Å] and, in addition, via a graphite-like π···π stacking of phenyl rings [Cg(Ph)···Cg(Ph) & sym(1−*x*, 2−*y*, −*z*): 3.7806(9) Å, interplanar separation 3.53 Å], C−H···π-ring interactions between the ferrocenyl unit and the five-membered purine ring of an adjacent molecule [C15−H15···Cg(Pur^5) & sym(2−*x*, $y-\frac{1}{2}$, $\frac{1}{2}-z$): Cg···C15 3.574(2) Å, C15−H15···Cg 143°] and C−H···N hydrogen bonds [C8−H8···N1 & sym(*x*, 1+*y*, *z*): C8···N1 3.461(2) Å, C8−H8···N1 172°].

The presence of free amino group in adenines **3b** and **4b** markedly affects the solid-state packing, since the N−H···N hydrogen bonding becomes the prominent force towards molec-

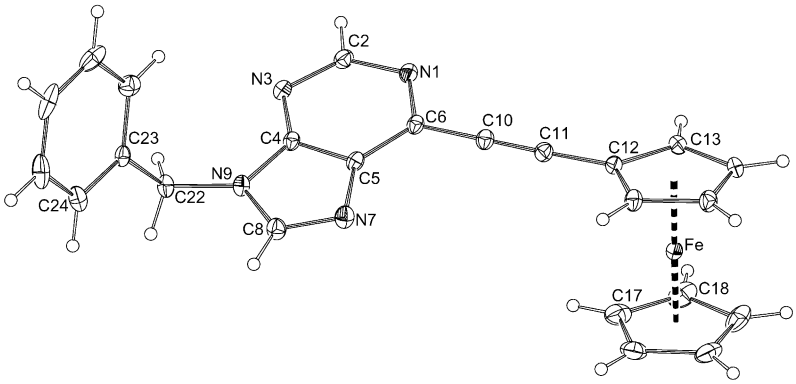

Figure 1. A view of the molecular structure of **3a** showing the atom-labelling scheme. Thermal motion ellipsoids are drawn at 30% probability level.

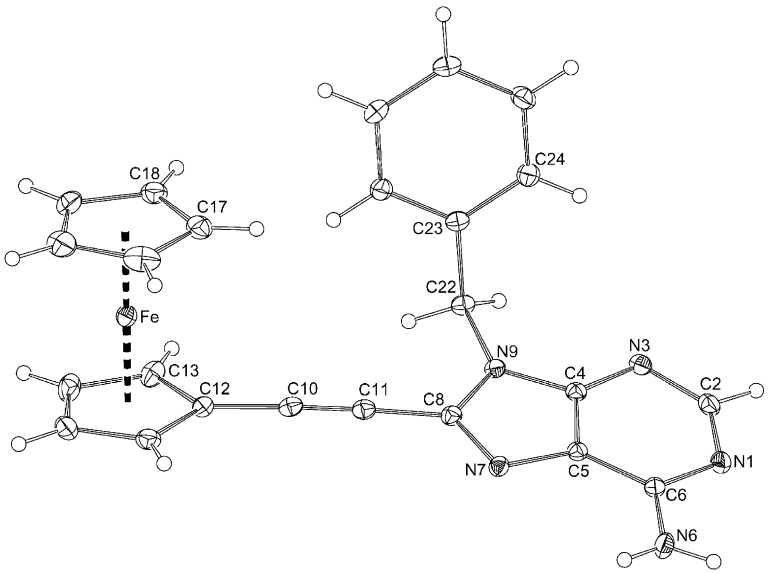

Figure 2. A view of the molecular structure of **3b** with the atom-labelling scheme. Thermal motion ellipsoids are drawn at 30% probability level.

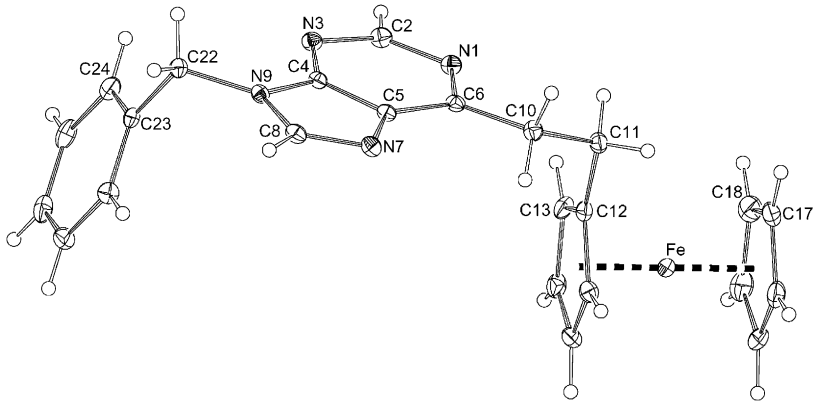

Figure 3. A view of the molecular structure of **4a** showing the atom-labelling scheme. Thermal motion ellipsoids are drawn at 30% probability level.

Table 1. Selected intermolecular distances and angles for **3a**, **4a**, and **3b** [Å and °].[a]

Compound	**3a**	**4a**	**3b**
x	6	6	8
N1–C2	1.339(2)	1.346(2)	1.342(2)
C2–N3	1.337(2)	1.332(2)	1.335(2)
N3–C4	1.331(2)	1.336(2)	1.345(2)
C4–C5	1.403(2)	1.397(2)	1.383(2)
C5–C6	1.399(2)	1.397(2)	1.411(2)
C6–N1	1.351(2)	1.346(2)	1.353(2)
C5–N7	1.388(2)	1.392(2)	1.382(2)
N7–C8	1.316(2)	1.315(2)	1.327(2)
C8–N9	1.364(2)	1.378(2)	1.382(2)
N9–C4	1.370(2)	1.370(2)	1.371(2)
C6–N6	–	–	1.334(2)
C*x*–C10	1.434(2)	1.503(2)	1.425(2)
C10–C11	1.199(2)	1.534(2)	1.188(2)
C11–C12	1.426(2)	1.503(2)	1.425(2)
N9–C22	1.467(2)	1.467(2)	1.466(2)
C*x*-C10-C11	178.4(2)	116.4(1)	176.1(2)
C10-C11-C12	178.4(2)	113.4(1)	176.9(2)
τ[b]	–	69.1(2)	–
Pur*y*,Cp1 [*y*]	20.53(7) [1]	86.27(8) [1]	19.2(1) [2]
Pur2, Ph	79.95(8)	71.35(8)	71.24(9)
Fe–Cg1	1.6385(7)	1.6432(7)	1.6486(9)
Fe–Cg2	1.6463(8)	1.6454(8)	1.653(1)
Cp1,Cp2	0.9(1)	1.0(1)	1.1(1)

[a] Plane definitions: Pur1: N1, C2, N3, N4, C5, C6; Pur2: C4, C5, N7, C8, N9; Cp1: C(12–16), Cp2: C(17–21), Ph: C(23–28). Cg1 and Cg2 are the centroids of the cyclopentadienyl rings Cp1 and Cp2, respectively. [b] τ = torsion angle C6-C10-C11-C12.

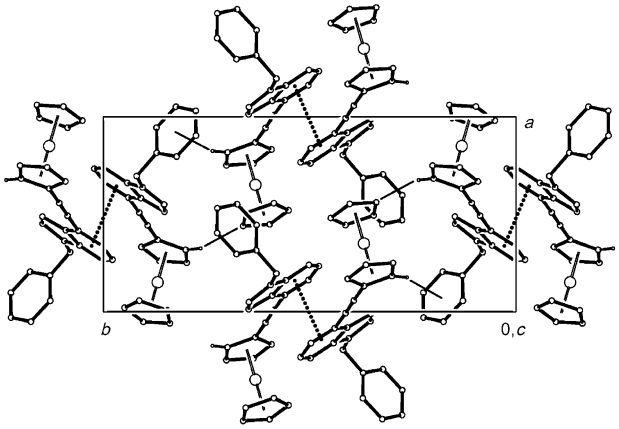

Figure 4. A drawing of the unit cell of **3a** as viewed along the crystallographic *c* axis. The most important intermolecular interactions are highlighted: π···π stacking as dotted lines and C–H···π interactions as solid lines.

ular assembly. Thus, the molecules of **3b** (Figure S2, Supporting Information) associate into dimers via centrosymmetric, double hydrogen bridges [N6–H92···N9 & sym(−*x*, 1−*y*, 2−*z*): N6···N9 2.962(2) Å, N6–H92···N9 162(2)°] while adjacent dimers are further interconnected by π···π interactions of aromatic rings, the shortest contact being the interaction between parallel five-membered purine rings [Cg(Pur^5)···Cg(Pur^5) & sym(1−*x*, 1−*y*, 2−*z*): Cg···Cg 4.352(1) Å], and C–H···π-ring bonding [C21–H21···Ph & sym(−*x*, 1−*y*, 1−*z*): C21···Cg(Ph) 3.705(2) Å, C21–H21···Ph 167°]. In accordance with the dominant role of N–H···N hydrogen bonding, the π···π and C–H···N interaction are less pronounced than in **3a** and **4a**, the participating groups being more distant than in the above compounds (for instance, the aromatic rings by as much as ca. 1 Å).

Crystal packing of **4b** is rather complicated, corresponding with a low crystallization ability of the compound. The triclinic unit accommodates two crystallographically independent but virtually identical molecules. Therefore, the increase in the occupancy of the asymmetric unit is likely to be accounted for intermolecular interactions. The crystal packing is shown in Figure 5 and the important interactions are summarized in Table 2. Similarly to **3b**, the molecules of **4b** associate into dimers formed by a molecule and its centrosymmetric counterpart via pairs of hydrogen bonds. However, unlike **3b** where only one amine hydrogen atom participates in hydrogen bonding, compound **4b** uses also the other amine hydrogen to form intermolecular N–H···N bonds, that crosslink the dimers of crystallographically independent molecules into infinite chains parallel to the crystallographic *b* axis. Thus, each molecule participates in four N–H···N iteractions: two forming the dimers and the remaining being responsible for dimer–dimer interactions.

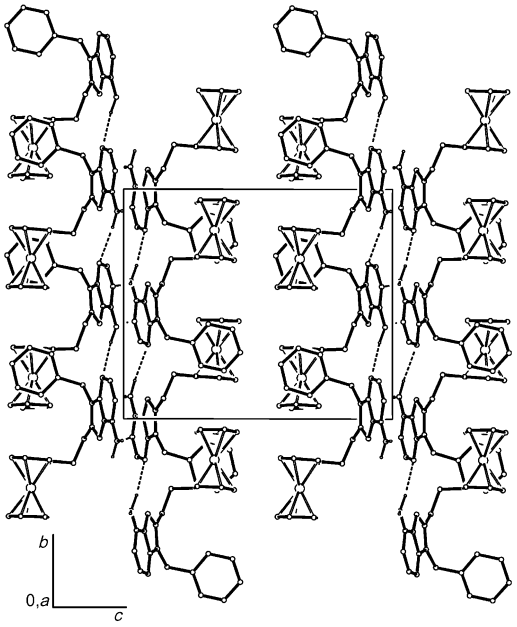

Figure 5. Crystal packing of **4b** as viewed along the crystallographic *b* axis. For clarity, the hydrogen atoms except NH are omited and hydrogen bonds are indicated as dashed lines.

Table 2. A listing of the major intermolecular interactions for **4b** [Å and °].[a]

Hydrogen bonding		
D−H···A	D···A	D−H···A
N6-H81···N1 & sym($2-x$, $-y$, $-z$)[b]	2.87(1)	177
N56-H91···N51 & sym($1-x$, $1-y$, $2-z$)[b]	2.93(1)	172
N6-H82···N53 & sym($1-x$, $1-y$, $1-z$)[c]	3.16(1)	152
N56-H92···N3 & sym($1-x$, $-y$, $1-z$)[c]	3.10(1)	156
C2-H2···N57 & sym($1-x$, $-y$,$1-z$)[c]	3.45(1)	149
π···π stacking		
	Cg···Cg	interplanar distance
$Pur^5(1)$···$Pur^5(1)$ & sym($1-x$, $-y$, $-z$)	3.387(5)	3.33
$Pur^5(2)$···$Pur^5(2)$ & sym($-x$, $1-y$, $2-z$)	3.511(5)	3.43
C−H···π-ring interactions		
	C···Cg	C−H···Cg
C10-H10B···$Pur^6(1)$ & sym($1-x$, $-y$, $-z$)	3.40(1)	152
C60-H60a···$Pur^6(1)$ & sym($-x$, $1-y$, $2-z$)	3.43(1)	156
C27-H27···$Cp^2(1)$ & sym(x, $y-1$, z)	3.47(1)	163

[a] Pur^5 and Pur^6 are five- and six-membered purine rings, respectively, and Cp^2 stands for the unsubstituted cyclopentadinenyl ring. The number, which follows parentheses, indicates the molecule (1,2). [b] Association into dimers. [c] Cross-linking of the H-bonded dimers.

The solid-state assembly of **4b** is further supported by offset π···π stacking of five-membered purine rings in centrosymmetrically related molecules [Cg···Cg 3.387(5) and 3.511(5) Å for pairs formed up by molecules 1 and 2, respectively] and some C−H···π-ring interactions (see Table 2). In summary, the crystal packing of **4b** is a columnar assembly of polar, hydrogen-bonded (purine) and non-polar parts (phenyl and ferrocenyl groups) [Note: the ferrocene units are nearly parallel and stacked into columns, though distant; the distance of their π-rings are ca. 5.7 and 5.9 Å].

Electrochemistry: The experimentally followed electrochemical response is a diffusion controlled one-electron reversible oxidation of the ferrocene system to ferricinium cation (Figures 6 and 7). The results are summarized in Table 3. The oxidation potentials of compounds **3a–c** are about 200 mV more positive than that of unsubstituted ferrocene whereas compounds **4a–c** are oxidized more easily than ferrocene itself. The oxidation potentials of the studied compounds and the difference in the oxidation potentials between these two series reflect the properties of the purine nucleus and the ferrocene-linking group.

Table 3. Voltammetric data for compounds **3** and **4** and comparison with model compounds.

Compound	$E_{1/2}$[a] (V, vs Fc/Fc^+)	$(E_{pc} + E_{pa})/2$[b] (V, vs Fc/Fc^+)
3a	0.205	0.205
4a	−0.043	−0.045
3b	0.210	0.210
4b	−0.035	−0.033
3c	0.165	0.167
4c	−0.062	−0.060
1	0.150	0.153
FcEt	−0.061[c]	–

[a] Data from voltammetry on rotating Pt-disc electrode. [b] Data from cyclic voltammetry on stationary Pt-disc electrode. E_{pc} and E_{pa} are cathodic and anodic peak potentials, respectively. [c] Data taken from ref. [16].

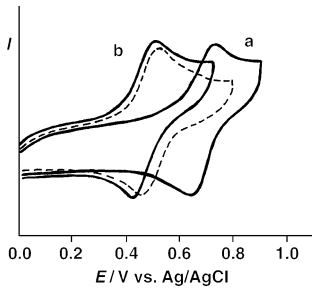

Figure 6. Cyclic voltammetric curves of compounds **3b** (curve a), **4b** (curve b) and ferrocene (dashed line). For conditions see Experimental Section.

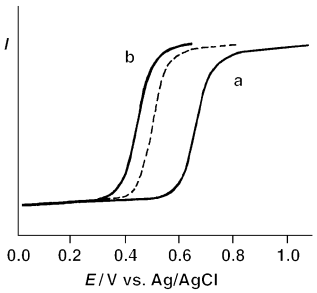

Figure 7. Voltammetric curves of compounds **3c** (curve a), **4c** (curve b) and ferrocene (dashed line). For conditions see Experimental section.

Influence of the bridge is evident from a comparison with two model compounds **1** and FcEt: alkyne **1** is oxidized at higher potentials than ferrocene (by ca. 150 mV) due to the electron-withdrawing nature of the triple bond that lowers electron density at iron and thus shifts the oxidation potential towards more positive values. On the other hand, FcEt is oxidized by about 60 mV more easily than ferrocene, reflecting an electron-donating effect of the alkyl group. The difference between these two potentials (0.214 V) represents approximately the contribution of the bridge to the oxidation potentials as compared to **3a–4a**, **3b–4b**, and **3c–4c** pairs, respectively.

The differences in oxidation potentials within series **3a–c** and **4a–c** can be accounted for an electronic influence of the parent heterocycle onto the ferrocene unit relayed via the bridge. In the case of **3a–c**, the electronic coupling is apparently enabled by the conjugated alkyne bridge,[14] while the non-conjugated ethane-1,2-diyl bridge in compounds **4a–c** reduces the influence of the purine moiety (although the oxidation potentials of **4a–c** are quite similar, they still follow the same trend as their unsaturated analogues **3a–c**, this indicates that the electronic communication is not disrupted completely by the saturated bridge). The difference in oxidation potentials of compounds **3b** and **3c** is quite substantial and does not reflect the general differences in electron densities in positions 2 and 8 on the purine nucleus. The pyrimidine moiety is known to behave as a more electron deficient part of the adenine unit[15] and thus one would anticipate a higher electron density on iron in compound **3b** than in **3c**. In fact, compound **3c** is oxidized more easily than **3b**. This discrepancy can be explained by theoretical calculation (see below).

Quantum chemistry calculations: Compounds **3b** and **3c** as well as the corresponding ferricinium cations ($\mathbf{3b}^+$ and $\mathbf{3c}^+$) were optimized by B3LYP method using 6-31G** base (Table 4, Figures S3 ad S4 in the Supporting Information). A comparison of the calculated structural data with the molecular parameters determined by X-ray crystallography for **3b** revealed only insignificant differences. The largest differences in interatomic distances were observed for the triple (calcd 1.216, found 1.188(2) Å) and the C6–N6 bonds (calcd 1.355, found 1.334(2) Å). As the ferrocene and heterocyclic plane in the calculated structure are nearly coplanar (dihedral angle Pur5,Cp1 2.7°; cf. Pur5,Ph 68.5° and values in Table 1), the former difference can be ascribed to an increased π-conjugation between adenine and ferrocene moieties as compared to the solid-state. On the other hand, the C6–N6 bond lengths likely reflect differences between isolated and hydrogen-bonded molecules.

Table 4. Calculated energies and ionization potentials (IP) for **3b** and **3c**.

Compound	E[a] [hartree]	IP[b] [eV]	IP[c] [eV]	Charge density[d] on ferrocene
3b	−2463.38581897	6.02	5.34	+0.0297
$\mathbf{3b}^+$	−2463.16476698			
3c	−2463.38093335	5.89	5.19	+0.0365
$\mathbf{3c}^+$	−2463.16459580			

[a] Total energies by B3LYP6-31G**. [b] Ionization potential as energy difference between the ferrocene derivative and its ferricinium cation. [c] Ionization potential by Koopmans theorem. [d] Sum of atomic charges for ferrocen unit by NBO method.

When analyzing the locations of frontier MO, we found that the HOMO orbitals in compounds **3b** and **3c** are localized at the ferrocene unit. This gives an evidence that oxidation should occur in both systems at the ferrocene. Ionization potentials (IP) were calculated both as an energy difference between the ferrocene derivative and ferricinium cation and by Koopmans theorem. The theoretical IP calculated by both methods confirm the experimental findings that compound **3c** is oxidized more easily than **3b**. Nevertheless, the calculations also confirmed the assumption that a higher electron density on ferrocene should occur in **3b** than in **3c**. These results clearly show that ionization potentials of ferrocene derivatives may not always be estimated just from electron densities on ferrocene unit.

Biological activity: Compounds **3** and **4** have been tested for their in vitro inhibition of cell growth in the following cell cultures: mouse leukemia L1210 cells (ATCC CCL 219), human promyelocytic leukemia HL60 cells (ATCC CCL 240), human cervix carcinoma HeLa S3 cells (ATCC CCL 2.2), and human T lymphoblastoid CCRF-CEM cell line (ATCC CCL 119). The results (Table 5) indicate that some of the compounds exhibit a considerable antiproliferative activity against L1210, HL60 and CCRF-CEM cell-lines but not against HeLa cells. The saturated derivatives **4a** and **4c** were the most active compounds in the whole series, having the IC_{50} values in micromolar concentrations. Such an activity is one to two orders of magnitude lower compared with the standard cytostatic 1-(β-D-2-deoxy-*erythro*-pentofuranosyl)-5-fluorouracil (FUDR). Nevertheless, these novel compounds represent a new lead structure in the design of antineoplastic agents.

Table 5. Cytostatic activity of compounds **3** and **4**.

Compound	IC_{50} [μmol L^{-1}][a]			
	L1210	HL60	HeLa S3	CCRF-CEM
3a	NA[b]	NA	NA	NA
3b	NA	NA	NA	13.7
3c	16.5	6.6	NA	6.7
4a	3.0	2.7	NA	2.6
4b	NA	NA	NA	8.0
4c	6.7	4.7	NA	3.8
FUDR[c]	0.012	0.012	>25	0.017

[a] Values are means of four experiments, standard deviation is given in parentheses; [b] NA = not active (inhibition of cell growth at 10 μM was lower than 30%); [c] 1-(β-D-2-deoxy-*erythro*-pentofuranosyl)-5-fluorouracil.

Conclusion

Sonogashira cross-coupling reactions of **1** with halopurines was confirmed to be a method of choice for the preparation of ferrocene-purine conjugates linked either via conjugated acetylene bridge or via non-conjugated ethane-1,2-diyl spacer. Such ferrocene-marked purines may be used as electrochemical markers of DNA or purine-based drugs detectable in very low concentrations. Electrochemical experiments proved that the ferrocene moiety is highly sensitive to the electronic changes on the purine ring and thus it may be expected that further studies could lead to the development of sensors based on these derivatives (studies in these directions are underway). Each of the three types of ferrocene–purine conjugates (linked via purine carbons 2, 6 or 8) has a distinct electrochemical response and thus such compounds may be used in investigations of modes of binding of some purines to proteins or nucleic acids (in each of them one position is blocked by the marker). Moreover, some of the studied purine derivatives displayed a considerable cytostatic effect.

Experimental Section

Unless otherwise stated, solvents were evaporated at 40°C/2 kPa and compounds were dried at 60°C/2 kPa. Melting points were determined on a Kofler block and are uncorrected. NMR spectra were measured on

a Bruker AMX-3 400 (400 MHz for ^{1}H and 100.6 MHz for ^{13}C nuclei) or a Bruker DRX 500 (500 MHz for ^{1}H and 125.8 MHz for ^{13}C) spectrometers. Tetramethylsilane was used as an internal standard. Mass spectra were measured on a ZAB-EQ (VG Analytical) spectrometer using FAB (ionization by Xe, accelerating voltage 8 kV, glycerol matrix). Cytostatic activity tests were performed as described in ref. [8a].

Et_3N was degassed in vacuo and stored over molecular sieves under argon. DMF was distilled from P_2O_5, degassed in vacuo and stored over molecular sieves under argon. Starting compounds **1**,[17] **2a**[18] and **2b**[19] were prepared according to the literature procedures. Other chemicals were purchased from commercial suppliers and used as received.

2-Chloro-9-benzyladenine (2c): A mixture of 2-chloroadenine (10 g, 59 mmol), K_2CO_3 (26 g, 188 mmol) and DMF (150 mL) was stirred at 50 °C for 1 h under Ar. After cooling to RT, benzyl chloride (12 mL) was added through a septum and the mixture was stirred at 90 °C for 18 h. The solvent was evaporated and the residue was purified by chromatography on a silica gel column (400 g, ethyl acetate/MeOH 10:0→8:2) to give the title compound accompanied by a complex mixture of the starting material and some side-products. The title compound was recrystallized from MeOH/toluene to yield colourless crystals (3.76 g, 25 %). M.p. 222–225 °C; ^{1}H NMR ([D$_6$]DMSO, 500 MHz): δ = 5.32 (s, 2H, CH_2Ph), 7.25–7.36 (m, 5H, H-arom.), 7.78 (s, 2H, NH_2), 8.24 (s, 1H, H-2); ^{13}C NMR ([D$_6$]DMSO, 125.8 MHz): δ = 46.22 (CH_2Ph), 117.71 (C-5), 127.32, 127.74, 128.68 (CH-arom.), 136.66 (C-*i*-arom.), 141.39 (CH-8), 150.52 (C-4), 153.09 (C-6), 156.76 (C-2); ^{1}H,^{13}C HMBC cross-peaks: CH_2 to *C*H-8 and *C*-4; EI MS: *m*/*z* (%): 259 (21) [M^+], 224 (6), 182 (8), 91 (100); exact mass (EI HR MS): calcd for $C_{12}H_{10}ClN_5$: 259.0625; found: 259.0615; elemental analysis calcd (%) for $C_{12}H_{10}ClN_5$ (259.7): C 55.50, H 3.88, N 26.97, Cl 13.65; found: C 55.62, H 3.96, N 26.64, Cl 14.00.

General procedure: **Cross-coupling of halopurines 2 with ethynylferrocene**

DMF (12 mL) and Et_3N (4 mL) were added through a rubber septum to an argon purged flask containing halopurine **2a–c** (2 mmol), ethynylferrocene (**1**) (465 mg, 2.2 mmol), CuI (50 mg, 0.25 mmol), and [Pd(PPh$_3$)$_4$] (100 mg, 0.087 mmol). After the mixture had been stirred at 120 °C for 16 h, the solvents were evaporated in vacuo and the residue purified by column chromatography on silica gel (150 g, ethyl acetate/light petroleum 1:2, and then ethyl acetate to ethyl acetate/MeOH 9:1).

9-Benzyl-6-(ferrocenylethynyl)purine (3a): Yield 86 %; dark red crystals; m.p. 158–161 °C (CH_2Cl_2/heptane); ^{1}H NMR ($CDCl_3$, 400 MHz): δ = 4.29 (s, 5H, H–Fc), 4.38 (s, 2H, H–Fc), 4.75 (s, 2H, H–Fc), 5.48 (s, 2H, CH_2Ph), 7.28–7.39 (m, 5H, H-arom.), 8.12 (s, 1H, C-8), 8.96 (s, 1H, H-2); ^{13}C NMR ($CDCl_3$, 100.6 MHz): δ = 47.36 (CH_2Ph), 62.43 (C-Fc), 70.08, 70.34, 72.72 (CH–Fc), 81.59, 100.22 (C≡C), 127.81, 128.66, 129.18 (CH-arom.), 133.62, 135.00 (C-*i*-arom. and C-5), 142.45 (C-6), 144.57 (CH-8), 151.52 (C-4), 152.86 (CH-2); IR ($CHCl_3$): $\tilde{\nu}$ = 2207, 1578, 1498, 1432, 1400, 1327 cm^{-1}; EI MS: *m*/*z* (%): 418 (73) [M^+], 353 (12), 327 (7), 121 (6), 91 (100); exact mass (EI HR MS): calcd for $C_{24}H_{18}FeN_4$: 418.0881; found: 418.0884; elemental analysis calcd (%) for $C_{24}H_{18}FeN_4$ (418.3): C 68.92, H 4.34, N 13.39; found: C 68.71, H 4.40, N 13.38.

9-Benzyl-8-(ferrocenylethynyl)adenine (3b): Yield 92 %; dark red crystals from EtOH/toluene; m.p. >215 °C (slow decomp.); ^{1}H NMR ([D$_6$]DMSO, 500 MHz): δ = 4.21 (s, 5H, H–Fc), 4.43 (t, 2H, *J* = 1.6 Hz, H–Fc), 4.68 (t, 2H, *J* = 1.6 Hz, H-Fc), 5.44 (s, 2H, CH_2Ph), 7.30–7.41 (m, 5H, H-arom.), 7.45 (s, 2H, NH_2), 8.21 (s, 1H, H-2); ^{13}C NMR ([D$_6$]DMSO, 125.8 MHz): δ = 46.01 (CH_2Ph), 61.34 (C-Fc), 69.95, 70.01, 71.68 (CH-Fc), 75.25, 95.27 (C≡C),118.67 (C-5), 127.37, 127.78, 128.69 (CH-arom.), 133.69, 136.73 (C-*i*-arom. and C-8), 153.66 (CH-2), 149.30, 155.65 (C-4, C-6); IR ($CHCl_3$): $\tilde{\nu}$ = 2223, 1633, 1588, 1575, 1464, 1327 cm^{-1}; UV/Vis (MeOH): λ_{max} (ε) = 449 (1300), 308 nm (24000); EI MS: *m*/*z* (%): 433 (100) [M^+], 368 (11), 342 (10), 121 (26), 91 (70); exact mass (EI HR MS): calcd for $C_{24}H_{19}FeN_5$: 433.0990; found: 433.1000; elemental analysis calcd (%) for $C_{24}H_{19}FeN_5$ (433.3): C 66.53, H 4.42, N 16.16; found: C 66.22, H 4.45, N 16.04.

9-Benzyl-2-(ferrocenylethynyl)adenine (3c): Reaction time 36 h, yield 37 % (40 % of starting compound was recovered), red crystals from EtOH/toluene; m.p. 138 °C (decomp); ^{1}H NMR ($CDCl_3$, 400 MHz): δ = 4.28 (brs, 7H, CH–Fc), 4.66 (brs, 2H, CH–Fc), 5.40 (s, 2H, CH_2Ph), 5.95 (s, 2H, NH_2), 7.26–7.40 (m, 5H, H-arom.), 7.72 (s, 1H, H-8); ^{13}C NMR ($CDCl_3$, 100.6 MHz): δ = 47.16 (CH_2Ph), 63.26 (C-Fc), 69.38, 70.11, 72.35 (CH–Fc), 85.69, 85.88 (C≡C), 118.62 (C-5), 127.96, 128.45, 129.08 (CH-arom.), 135.45 (C-*i*-arom.), 140.89 (CH-8), 147.20, 150.52, 155.26 (C-2, C-4, C-6); IR ($CHCl_3$): $\tilde{\nu}$ = 2217, 1627, 1586, 1444, 1384, 1362 cm^{-1}; UV/Vis (MeOH): λ_{max} (ε) = 449 (500), 366 (1400), 308 (8500); 265 nm (19800); EI MS: *m*/*z* (%): 433 (100) [M^+], 342 (7), 91 (26); exact mass (EI HR MS): calcd for $C_{24}H_{19}FeN_5$: 433.0990; found: 433.0980; elemental analysis calcd (%) for $C_{24}H_{19}FeN_5$ (433.3): C 66.53, H 4.42, N 16.16; found: C 66.20, H 4.40, N 15.95.

General procedure: **Hydrogenation of alkynylpurines 3**

A solution of an ethynylpurine **3** (1 mmol) in a mixture of dioxane (20 mL), ethanol (100 mL) and acetic acid (20 mL) was hydrogenated in the presence of 10 % Pd/C (150 mg) under atmospheric pressure for 36 h. The catalyst was filtered off, the mixture evaporated, and the residue purified by chromatography on a silica gel column (150 g, ethyl acetate/light petroleum 1:2, then ethyl acetate to ethyl acetate/MeOH 9:1).

9-Benzyl-6-(2-ferrocenylethyl)purine (4a): Yield 52 %; brownish oil that crystallized on standing; m.p. 127 °C (decomp); ^{1}H NMR ($CDCl_3$, 400 MHz): δ = 2.96 (dd, 2H, *J* = 8.4, 7.7 Hz, CH_2CH_2), 3.45 (dd, 2H, *J* = 8.4, 7.7 Hz, CH_2CH_2), 4.04 (s, 2H, H-Fc), 4.11–4.15 (s, 7H, H-Fc), 5.44 (s, 2H, CH_2Ph), 7.29–7.36 (m, 5H, H-arom.), 8.00 (s, 2H, H-8), 8.94 (s, 1H, H-2); ^{13}C NMR ($CDCl_3$, 100.6 MHz): δ = 28.14, 34.49 (CH_2CH_2), 47.24 (CH_2Ph), 67.20, 68.04, 68.49 (CH–Fc), 88.22 (C–Fc), 127.81, 128.55, 129.11 (CH-arom.), 132.44, 135.18 (C-5, C-*i*-arom.), 143.55 (CH-8), 152.61 (CH-2); 150.87 (C-4), 162.09 (C-6); IR ($CHCl_3$): $\tilde{\nu}$ = 1596, 1499, 1456, 1406, 1332 cm^{-1}; EI MS: *m*/*z* (%): 422 (100) [M^+], 357 (95), 279 (16), 224 (16), 91 (99); exact mass (EI HR MS): calcd for $C_{24}H_{22}FeN_4$: 422.1194 found: 422.1200; elemental analysis calcd (%) for $C_{24}H_{22}FeN_4$ (422.3): C 68.26, H 5.25, N 13.27; found: C 68.22, H 5.42, N 12.96.

9-Benzyl-8-(2-ferrocenylethyl)adenine (4b): Yield 71 %; yellow crystals from MeOH/toluene/heptane; m.p. 198 °C (decomp); ^{1}H NMR ($CDCl_3$, 500 MHz): δ = 2.75 (dd, 2H, *J* = 8.5, 7.3 Hz, CH_2CH_2), 2.90 (dd, 2H, *J* = 8.5, 7.3 Hz, CH_2CH_2), 3.98 (s, 2H, H–Fc), 4.04 (s, 5H, H–Fc), 4.05 (m, 2H, H–Fc), 5.26 (s, 2H, CH_2Ph), 5.69 (s, 2H, NH_2), 7.10–7.12 (m, 2H, H-arom.), 7.27–7.33 (m, 3H, H-arom.), 8.37 (s, 1H, H-2); ^{13}C NMR ($CDCl_3$, 125.8 MHz): δ = 27.75, 29.87 (CH_2CH_2), 45.59 (CH_2Ph), 67.58, 68.05, 68.52 (CH–Fc), 86.98 (C-Fc), 118.54 (C-5), 126.81, 128.00, 128.96 (CH-arom.), 135.97 (C-*i*-arom.), 152.51 (CH-2), 151.43, 152.83, 154.46 (C-4, C-6, C-8); IR ($CHCl_3$): $\tilde{\nu}$ = 1633, 1608, 1498, 1456, 1385, 1327 cm^{-1}; EI MS: *m*/*z* (%): 437 (70) [M^+], 372 (85), 281 (21), 121 (45), 91 (100); exact mass (EI HR MS): calcd for $C_{24}H_{23}FeN_5$: 437.1303 found: 437.1307; elemental analysis calcd (%) for $C_{24}H_{23}FeN_5$ (437.3): C 65.91, H 5.30, N 16.01; found: C 65.70, H 5.33, N 15.92.

9-Benzyl-2-(2-ferrocenylethyl)adenine (4c): Yield 56 %; orange crystals from MeOH/toluene/heptane; slow decomp. above 80 °C; ^{1}H NMR ($CDCl_3$, 400 MHz): δ = 2.89, 3.08 (2×brt, 2×2H, *J* = 7.6 Hz, CH_2CH_2), 4.03–4.15 (brm, 9H, H-Fc), 5.36 (s, 2H, CH_2Ph), 5.70 (s, 2H, NH_2), 7.20–7.40 (brm, 5H, H-arom.), 7.69 (s, 1H, H-8); ^{13}C NMR ($CDCl_3$, 100.6 MHz): δ = 28.52, 40.51 (CH_2CH_2), 47.05 (CH_2Ph), 67.05, 68.10, 68.46 (CH–Fc), 88.82 (C-Fc), 117.76 (C-5), 127.95, 128.30, 128.97 (CH-arom.), 135.90 (C-*i*-arom.), 139.95 (CH-8), 151.03, 155.17 (C-4, C-6), 165.43 (C-2); IR ($CHCl_3$), $\tilde{\nu}$ = 1626, 1592, 1498, 1456, 1391, 1339 cm^{-1}; EI MS: *m*/*z* (%): 437 (100) [M^+], 372 (62), 294 (29), 121 (36), 91 (80); exact mass (EI HR MS); calcd for $C_{24}H_{23}FeN_5$: 437.1303; found: 437.1306; elemental analysis calcd (%) for $C_{24}H_{23}FeN_5$ (437.3): C 65.91, H 5.30, N 16.01; found: C 65.84, H 5.48, N 15.73.

X-Ray crystallography: Single-crystals were grown by crystallization from dichloromethane/hexane (**3a**: ruby red prism, 0.27×0.32×0.40 mm^3; **4a**: orange-yellow block, 0.28×0.28×0.30 mm^3; **3b**: rusty orange block, 0.13×0.25×0.33 mm^3). Repeated attempts at obtaining single crystals of **4b** resulted only in thin, layered crystalline aggregates. Finally, a very thin yellow plate (0.30×0.13×0.03 mm^3) was selected after crystallizatiom from MeOH/toluene and subjected to crystallographic analysis. Although the obtained data and, consequently, the structure determination are of a rather low precision (see *R* values and residual electron density in Table 6), the overall chemical picture, and particularly the crystal packing, which shows interresting features very different from other studied compounds, are unambiguous.

Full-set diffraction data ($\pm h \pm k \pm l$) for all compounds were collected on an Nonius KappaCCD diffractometer equipped with Cryostream Cooler (Oxford Cryosystems) at 150(2) K using graphite monochromatized Mo$_{K\alpha}$

radiation ($\lambda = 0.71073$ Å) and analyzed with HKL program package.[20] No absorption correction was applied. The structures were solved by direct methods (SIR97, ref. [21]) and refined by weighted full-matrix least squares procedure on F^2 (SHELXL97, ref. [22]). All non hydrogen atoms were refined with anisotropic thermal motion parameters. Hydrogen atoms at the amine nitrogen N6 in **3a** were identified on difference electron density maps and freely refined. All other hydrogen atoms were included in the calculated positions [C–H bond lengths 0.97 (methylene), and 0.93 (aromatic) Å; N–H in **4b** 0.86 Å] and assigned $U_{iso}(H) = 1.2\,U_{eq}(C)$ or $U_{iso}(H) = 1.5\,U_{eq}(N)$. The final geometric calculations were carried out with Platon program.[23] Relevant crystallographic data and structure refinement parameters are summarized in Table 6.

CCDC-216296 (**3a**), -216297 (**4a**), -216298 (**3b**), and -216299 (**4b**) contain the supplementary crystallographic data for this paper. These data can be obtained free of charge via www.ccdc.cam.ac.uk/conts/retrieving.html (or from the Cambridge Crystallographic Data Centre, 12 Union Road, Cambridge CB2 1EZ, UK; fax: (+44) 1223–336–033; or deposit@ccdc.cam.uk).

Electrochemistry: The electrochemical measurements were performed using the potentiostat LP3 (Laboratorní přístroje, Prague) in a standard three-electrode mode. The "Metrohm type" cell was filled with 0.1 M Bu_4NPF_6 in acetonitrile (10 mL) and deaerated by argon. The concentration of studied compounds was 1.10^{-5} M. Platinum rotated disk electrode (RDE) with diameter 1.5 mm or platinum stationary disk electrode were used as working electrodes, platinum wire as auxiliary electrode and a saturated calomel electrode (SCE) with a non-aqueous bridge filled with acetonitrile solution of Bu_4NPF_6 solution served as the reference electrode. Two techniques were used: voltammetry at rotating electrode (1000 min^{-1}; $v = 10\ mV\,s^{-1}$) and cyclic voltammetry (CV) at the stationary electrode ($v = 200\ mV\,s^{-1}$). All potentials are given relative to ferrocene/ferricinium couple.

Calculations: The geometry of both molecules (**3b** and **3c**) was optimized using the DFT/B3LYP method with 6-31G** basis set. Natural bond orbital analysis yielding charges and electron density distributions was performed for both optimized structures at the same theoretical level. Ionization potential was determined using the Koopmans theorem. Further, it was also calculated as a difference between the energy of the parent (neutral) system and respective cation radical. The geometry of radical cations of both structures was again optimized at the DFT/B3LYP level using the 6-31G** basis set. All calculations were performed with Gaussian 98.[24]

Acknowledgement

This work is a part of research project Z4 055 905. It was supported by the Grant Agency of the Czech Republic (grant 203/03/0035 (to M.H.) and 203/99/M037 (to I.C.)), by the grant Agency of the Academy of Sciences of the Czech Republic (grant A4040304 (to J. L.) and B4055201 to (M. H.)) and by Sumika Fine Chemicals, Co. Ltd. (Osaka, Japan). Financial support by the Center of Complex Molecular Systems and Biomolecules (Project LN00A032 of MSMT CR) and by the 6th framework EU (grant CIDNA, P. No. 505669-1) is also acknowledged. The authors also thank Dr. Hana Dvořáková for measurement and interpretation of NMR spectra and Mrs. Kamila Havlíčková for technical assistance.

[1] Review: M. Hocek, *Eur. J. Org. Chem.* **2003**, 245–254.

[2] a) Review: C. E. Müller, *Curr. Med. Chem.* **2000**, *7*, 1269–1288; b) recent example: R. Volpini, S. Constanzi, C. Lambertucci, S. Taffi, S. Vittori, K.-N. Klotz, G. Cristalli, *J. Med. Chem.* **2002**, *45*, 3271–3279.

[3] a) C. E. Müller, B. Stein, *Curr. Pharm. Des.* **1996**, *2*, 501–530; b) C. E. Müller, *Exp. Opin. Ther. Pat.* **1997**, *7*, 419–440; c) M. T. Shamim, D. Ukena, W. L. Padget, J. W. Daly, *J. Med. Chem.* **1989**, *32*, 1231–1237.

[4] R. Volpini, S. Constanzi, C. Lambertucci, S. Vittori, K.-N. Klotz, A. Lorenzen, G. Cristalli, *Bioorg. Med. Chem. Lett.* **2001**, *11*, 1931–1934.

[5] a) A. Brathe, L.-L. Gundersen, F. Rise, A. B. Eriksen, A. V. Vollsnes, L. Wang, *Tetrahedron* **1999**, *55*, 211–228; b) G. Andresen, L.-L. Gundersen, J. Nissen-Meyer, F. Rise, B. Spilsberg, *Bioorg. Med. Chem. Lett.* **2002**, *12*, 567–569.

[6] A. Brathe, G. Andresen, L.-L. Gundersen, K. E. Malterud, F. Rise, *Bioorg. Med. Chem.* **2002**, *10*, 1581–1586.

[7] a) A. K. Bakkestuen, L.-L. Gundersen, G. Langli, F. Liu, J. M. J. Nolsøe, *Bioorg. Med. Chem. Lett.* **2000**, *10*, 1207–1210; b) A. Brathe, G. Andresen, L.-L. Gundersen, K. E. Malterud, F. Rise, *Bioorg. Med. Chem.* **2002**, *10*, 1581–1586.

[8] a) M. Hocek, A. Holý, I. Votruba, H. Dvořáková, *J. Med. Chem.* **2000**, *43*, 1817–1825; b) M. Hocek, A. Holý, I. Votruba, H. Dvořáková, *Collect. Czech. Chem. Commun.* **2001**, *66*, 483–499; c) M. Hocek, A. Holý, H. Dvořáková, *Collect. Czech. Chem. Commun.* **2002**, *67*, 325–335.

Table 6. Crystallographic data, data collection and structure refinement for **3a**, **4a**, **3b**, and **4b**.

Compound	**3a**	**4a**	**3b**	**4b**
formula	$C_{24}H_{18}FeN_4$	$C_{24}H_{22}FeN_4$	$C_{24}H_{19}FeN_5$	$C_{24}H_{23}FeN_5$
M_w [g mol^{-1}]	418.27	422.31	433.29	437.32
crystal system	monoclinic	monoclinic	triclinic	triclinic
space group	$P2_1/n$ (no. 14)	$P2_1/c$ (no. 14)	$P\bar{1}$ (no. 2)	$P\bar{1}$ (no. 2)
a [Å]	9.6956(2)	10.2217(1)	9.5820(2)	10.4150(5)
b [Å]	19.6608(2)	7.8573(1)	10.6997(2)	13.1110(6)
c [Å]	10.3548(1)	23.7597(3)	11.2350(2)	15.5310(9)
α [°]	90	90	112.822(1)	89.836(2)
β [°]	107.6503(8)	100.750(1)	105.1938(7)	79.231(3)
γ [°]	90	90	99.5319(7)	88.469(3)
V [Å^3]	1880.95(5)	1874.77(4)	977.24(3)	2082.7(2)
Z	4	4	2	4
ρ_{calcd} [g mL^{-1}]	1.477	1.496	1.473	1.395
$2\theta_{max}$ [°]	55.0	55.0	55.0	52.0
$\mu(Mo_{K\alpha})$ [mm^{-1}]	0.820	0.823	0.793	0.745
no. collected diffrns	30951	29219	16165	27159
no. unique diffrns	4294	4290	4453	8144
no. observed diffrns	3896	3805	3957	6025
no. parameters	262	262	279	545
R, wR obsd. diffrns [%][b]	2.71, 6.86	2.87, 7.08	2.99, 6.97	11.3, 29.9
R, wR all data [%][b]	3.09, 7.10	3.44, 7.38	3.60, 7.26	14.2, 31.2
$\Delta\rho$ [e Å^{-3}]	0.31, −0.37	0.33, −0.40	0.28, −0.34	1.87, −0.88

[a] Diffractions with $I_o > 2\sigma(I_o)$. [b] Definitions: $R(F) = \Sigma\,||F_o| - |F_c||/\Sigma\,|F_o|$, $wR(F^2) = [\Sigma(w(F_o^2 - F_c^2)^2)/(\Sigma w(F_o^2)^2)]^{1/2}$.

[9] a) M. Hocek, I. Votruba, *Bioorg. Med. Chem. Lett.* **2002**, *12*, 1055–1057; b) M. Hocek, H. Dvořáková, I. Císařová, *Collect. Czech. Chem. Commun.* **2002**, *67*, 1560–1578; c) M. Hocek, I. Votruba, H. Dvořáková, *Tetrahedron* **2003**, *59*, 607–611.
[10] C. J. Yu, H. Wang, Y. J. Wan, H. Yowanto, J. C. Kim, L. H. Donilon, C. L. Tao, M. Strong, Y. C. Chong, *J. Org. Chem.* **2001**, *66*, 2937–2942.
[11] C. J. Yu, Y. J. Wan, H. Yowanto, J. Li, C. L. Tao, M. D. James, C. L. Tan, G. F. Blackburn, T. J. Meade, *J. Am. Chem. Soc.* **2001**, *123*, 11155–11161.
[12] a) P. Meunier, I. Ouattara, B. Gautheron, J. Tirouflet, D. Camboli, J. Besancon, *Eur. J. Med. Chem.* **1991**, *26*, 351–362; b) E. Bucci, L. De Napoli, G. Di Fabio, A. Messere, D. Montesarchio, A. Romanelli, G. Piccialli, M. Varra, *Tetrahedron* **1999**, *55*, 14435–14450; c) C. J. Yu, H. Yowanto, Y. J. Wan, T. J. Meade, Y. Chong, M. Strong, L. H. Donilon, J. F. Kayyem, M. Gozin, G. F. Blackburn, *J. Am. Chem. Soc.* **2000**, *122*, 6767–6768; d) A. R. Pike, L. C. Ryder, B. R. Horrocks, W. Clegg, M. R. J. Elsegood, B. A. Connolly, A. Houlton, *Chem. Eur. J.* **2002**, *8*, 2891–2899; e) W. A. Wlassoff, G. C. King, *Nucleic Acids Res.* **2002**, *30*, e58; f) F. Patolsky, Y. Weizmann, I. Willner, *J. Am. Chem. Soc.* **2002**, *124*, 770–772.
[13] E. Coutouli-Argyropoulou, M. Tsitabani, G. Petrantonakis, A. Terzis, C. Raptopoulou, *Org. Biomol. Chem.* **2003**, *1*, 1382–1388.
[14] P. Štěpnička, L. Trojan, J. Kubišta, J. Ludvík, *J. Organomet. Chem.* **2001**, *637–639*, 291–299.
[15] J. Šponer, J. Leszczynski, P. Hobza, *J. Phys. Chem.* **1996**, *100*, 5590–5596.
[16] G. L. K. Hoh, W. E. Mc Ewen, J. Kleinberg, *J. Am. Chem. Soc.* **1961**, *83*, 3949–3953.
[17] M. Rosenblum, N. Brawn, J. Papenmeier, M. Applebaum, *J. Organomet. Chem.* **1966**, *6*, 173–180.
[18] L.-L. Gundersen, A. K. Bakkestuen, A. J. Aasen, H. øveras, F. Rise, *Tetrahedron* **1994**, *50*, 9743–9756.
[19] M. Havelková, D. Dvořák, M. Hocek, *Synthesis* **2001**, 1704–1710.
[20] Z. Otwinowski, W. Minor, HKL Denzo and Scalepack program package by Nonius BV, Delft, **1997**. For a reference see: Z. Otwinowski, W. Minor, *Methods Enzymol.* **1997**, *276*, 307–326.
[21] A. Altomare, M. C. Burla, M. Camalli, G. L. Cascarano, C. Giacovazzo, A. Guagliardi, A. G. G. Moliterni, G. Polidori, R. Spagna, *J. Appl. Crystallogr.* **1999**, *32*, 115–119.
[22] G. M. Sheldrick, SHELXL97, Program for Crystal Structure Refinement from Diffraction Data, University of Göttingen, Göttingen, **1997**.
[23] A. L. Spek, Platon-a multipurpose crystallographic tool (2001); see: http://www.cryst.chem.uu.nl/platon/.
[24] Gaussian 98, Revision A.11.4, M. J. Frisch, G. W. Trucks, H. B. Schlegel, G. E. Scuseria, M. A. Robb, J. R. Cheeseman, V. G. Zakrzewski, J. A. Montgomery, Jr., R. E. Stratmann, J. C. Burant, S. Dapprich, J. M. Millam, A. D. Daniels, K. N. Kudin, M. C. Strain, O. Farkas, J. Tomasi, V. Barone, M. Cossi, R. Cammi, B. Mennucci, C. Pomelli, C. Adamo, S. Clifford, J. Ochterski, G. A. Petersson, P. Y. Ayala, Q. Cui, K. Morokuma, N. Rega, P. Salvador, J. J. Dannenberg, D. K. Malick, A. D. Rabuck, K. Raghavachari, J. B. Foresman, J. Cioslowski, J. V. Ortiz, A. G. Baboul, B. B. Stefanov, G. Liu, A. Liashenko, P. Piskorz, I. Komaromi, R. Gomperts, R. L. Martin, D. J. Fox, T. Keith, M. A. Al-Laham, C. Y. Peng, A. Nanayakkara, M. Challacombe, P. M. W. Gill, B. Johnson, W. Chen, M. W. Wong, J. L. Andres, C. Gonzalez, M. Head-Gordon, E. S. Replogle, J. A. Pople, Gaussian, Inc., Pittsburgh PA, 2002.

Received: October 14, 2003 [F5621]

